REPORT DOCUMENTATION PAGE

Form Approved
OMB No. 0704-0188

1. REPORT DATE *(DD-MM-YYYY)*
27-12-2002

2. REPORT TYPE
Technical Paper

3. DATES COVERED *(From - To)*

4. TITLE AND SUBTITLE

Swirl Coaxial Injector Development

5a. CONTRACT NUMBER

5b. GRANT NUMBER

5c. PROGRAM ELEMENT NUMBER

6. AUTHOR(S)
R. K. Cohn, P. A. Strakey, R.W.. Bates, J.A. Muss, C.W. Johnson
D.G. Talley,

5d. PROJECT NUMBER
3058

5e. TASK NUMBER
RF9A

5f. WORK UNIT NUMBER

7. PERFORMING ORGANIZATION NAME(S) AND ADDRESS(ES)

Air Force Research Laboratory (AFMC)
AFRL/PRSS
1 Ara Drive.
Edwards AFB, CA 93524-7013

Sierra Engineering Inc.
Carson City, NV

8. PERFORMING ORGANIZATION REPORT NUMBER

AFRL-PR-ED-TP-2002-324

9. SPONSORING / MONITORING AGENCY NAME(S) AND ADDRESS(ES)

Air Force Research Laboratory (AFMC)
AFRL/PRS
5 Pollux Drive
Edwards AFB CA 93524-7048

10. SPONSOR/MONITOR'S ACRONYM(S)

11. SPONSOR/MONITOR'S NUMBER(S)
AFRL-PR-ED-TP-2002-324

12. DISTRIBUTION / AVAILABILITY STATEMENT

Approved for public release; distribution unlimited.

13. SUPPLEMENTARY NOTES

14. ABSTRACT

20030227 165

15. SUBJECT TERMS

16. SECURITY CLASSIFICATION OF:			**17. LIMITATION OF ABSTRACT**	**18. NUMBER OF PAGES**	**19a. NAME OF RESPONSIBLE PERSON**
					Leilani Richardson
a. REPORT	**b. ABSTRACT**	**c. THIS PAGE**	A		**19b. TELEPHONE NUMBER** *(include area code)*
Unclassified	Unclassified	Unclassified			(661) 275-5015

Standard Form 298 (Rev. 8-98)
Prescribed by ANSI Std. 239.18

JON 3058 RF9A
KTR
WU

MEMORANDUM FOR PRS (In-House Publication)

FROM: PROI (STINFO)

27 Dec 2002

SUBJECT: Authorization for Release of Technical Information, Control Number: **AFRL-PR-ED-TP-2002-324**
Rich Cohn (PRSA) et al., "Swirl Coaxial Injector Development"

AIAA Aerospace Sciences Conference
(Reno, NV, 6-9 January 2003) (Deadline: 06 Jan 2003)

(Statement A)

SWIRL COAXIAL INJECTOR DEVELOPMENT

R.K. Cohn, P.A. Strakey, R.W. Bates and D.G. Talley
Air Force Research Laboratory, Edwards AFB, CA

J.A. Muss and C.W. Johnson
Sierra Engineering Inc., Carson City, NV

ABSTRACT

Sierra Engineering and the Air Force Research Laboratory Propulsion Directorate, have undertaken a program to develop gas-centered, swirl coaxial injectors. This injector design will be used in the multi-element Advanced Fuels Tester (AFT) engine to test a variety of hydrocarbon propellants. As part of this program, a design methodology is being developed which will be applicable to future injector design efforts. The methodology combines cold flow data, acquired in the AFRL High Pressure Injector Flow facility, uni-element hot fire data, collected in AFRL Test Cell EC-1, and a computational effort conducted at University of Alabama-Birmingham, to identify key design features and sensitivities. Only results from the experimental effort will be presented in this work.

Three different gas-centered swirl coaxial element concepts are being studied: a converging design, a diverging design, and a pre-filming design. The cold flow experiments demonstrated that all three classes of elements produced an extremely dense, solid cone spray, with the highest mass density in the center. The atomization of all of these injectors was excellent, producing mean drop sizes 1/3 to 1/4 of that typically measured for shear coaxial elements operating under similar conditions. Uni-element hot fire testing has found that the converging designs produce C* efficiencies in excess of 90% over a wide-range of mixture ratios and pressure conditions. Near the design pressure, efficiencies exceeding 96% have been measured. In the diverging designs, a chamber oscillation of near 200 Hz has been noted. The cause of this oscillation is under investigation.

INTRODUCTION

Sierra Engineering and AFRL are in the process of developing liquid rocket engine injectors. The purpose of this work is two-fold. First, the development of rocket engine injectors to study the performance of various hydrocarbon fuels with gaseous oxygen (GOX) as an oxidizer. In order to meet this goal, the injector needs to be insensitive to fuel properties, as well as the mixture ratio. It should be noted that we are concentrating our efforts on conditions in which the fuel is supercritical upon injection. Secondly, we are trying to develop a design methodology which will aid in the development of future rocket engine injectors.

The basic injector design includes a gas-centered swirl coaxial injector element similar, in principle, to the injection element used in many Russian flight engines. As the name implies, this element concept directs the gaseous propellant (GOX) through the center of the element with the liquid propellant injected along the periphery of the element. The liquid propellant is injected tangentially along the element wall, producing a swirling liquid film. The gas-centered swirl coaxial injection element differs from the swirl coaxial elements previously demonstrated by Aerojet (2) and Pratt & Whitney (3), amongst others, in that these latter designs swirl the central liquid propellant and shroud the liquid with a coaxially injected gas. The gaseous propellant may also include a swirl component in these designs.

The motivation for the radically different injector design approach can be found in basic combustion chemistry. Previous domestic (USA) applications of swirl coaxial injectors to rocket engines have been primarily to gaseous fuel/liquid oxidizer systems; as such the approach was to shroud the liquid oxidizer with gaseous fuel, the oxidizer, in theory, will be completely encapsulated, and ultimately consumed by the gaseous fuel. This prevents free oxidizer from reaching the combustion chamber wall. In contrast, the AFT hardware, as well as the Russian engines that employ the gas-centered injection element, utilizes a gaseous oxidizer and liquid fuel. Therefore, the gas-centered swirl coaxial injector also encapsulates the oxidizer with fuel. In both cases, atomization of the liquid propellant is accomplished through a combination of conventional swirl atomization, i.e., thinning of a liquid sheet until surface instabilities initiate ligamentation and ultimately atomization, and shear induced by the high-speed adjacent gaseous propellant.

The gas-centered swirl coaxial element also offers potential to increase the thrust-per-element which can potentially reduce both fabrication and

---

operating costs. The largest US oxygen-hydrocarbon engines, which utilize conventional impinging elements, achieve a thrust-per-element on the order of 2,500 lb_f (4). In contrast, the Russian RD-170 engine, utilizing this type of element, has a thrust-per-element in excess of 6,000 lb_f.

While the gas-centered swirl coaxial injector appears to be well suited for this project as well as other future oxygen-hydrocarbon applications, there is a dearth of design guidelines and test data for this type of element in the US. Liquid swirl-type injectors are commonly used in industrial applications that include industrial boilers, gas turbines and spray drying. They have also been the subject of numerous design monographs, such as References 5 and 6. However, these applications address sprays into a quiescent or co-flowing gas, with the gas typically being the oxidizer. This application is more consistent with the traditional liquid-centered swirl coaxial design. Lefebvre describes several applications where gas is introduced on both the inside and outside of the liquid fuel sheet with the intention of enhancing atomization (5), but, as noted above, this application is designed to uniformly distribute the liquid spray within the gaseous oxidizer. These approaches can give some guidance to the design and operating characteristics of a gas-centered swirl coaxial injector, but it is not directly applicable design data.

Sierra Engineering has joined with the Air Force Research Laboratory, Propulsion Directorate, Aerophysics Branch (AFRL/PRSA) to systematically investigate the sensitivity of various design parameters on the operating characteristics of gas-centered swirl coaxial injection elements. The program utilizes a combination of uni-element cold flow and uni-element hot fire tests along with computational fluid dynamic (CFD) calculations, to develop a design approach for the AFT injector element. The following sections describe the test hardware designs, the cold flow test results, and preliminary hot fire test results. The results of the CFD calculations will not be discussed in the present work.

HARDWARE DESIGN

The basic gas-centered swirl coaxial element design can be conceptualized as a straight-run post for the oxidizer. The post includes a discrete set of fuel injection orifices near the downstream exit of the oxidizer post. The orifices are oriented to generate swirling fuel around the periphery. The fuel film generated around the post periphery is subject to a combination of cross-flow shear and centrifugal forces. As the liquid exits the tip of the oxidizer post, centrifugal forces create a conically expanding sheet of liquid that thins due to continuity. This liquid sheet film also interacts with the central oxygen gas jet, which typically entrains the liquid fluid, transporting the resultant spray downstream. The parameters that can be varied in this design include the number of fuel injection orifices, the axial location of the orifices relative to the final injection location and most importantly the post geometry near the fuel injection orifices. Three basic injector concepts were identified for comparative evaluation, the diverger, the converger and the pre-filmer, as shown schematically in Figure 1, Figure 2 and Figure 3, respectively.

The diverger design injects the fuel downstream of a sudden expansion, with the expansion having a characteristic expansion angle. The characterized dimensions of the diverger, shown in Figure 1, are the oxidizer post diameter (A), the diameter of the sudden expansion (E), the length of the expansion section (C) and the divergence angle (θ). Additional parameters are the diameter (D) and quantity of fuel injection orifices. Several of these characteristic dimensions should also be considered as ratios: the expansion ratio (E/A), expansion distance (C/A) and the fuel orifice diameter to expansion step (2D/[E-A]). A set of five parametric diverger element designs was developed, as described in Table 1.

The converger element design is loosely based on the main chamber injection element used in several Russian staged-combustion engines. The fuel is tangentially injected into the main oxidizer post. Then, the post necks-down to accelerate both the liquid and gaseous flows. The characterized dimensions of the converger, shown in Figure 2, are the oxidizer post diameter (A) and the diameter (E) and length (C) of the necked-down section. Again, additional parameters are the diameter (D) and quantity of fuel injection orifices. The characteristic dimensions that should be considered as ratios are the contraction ratio (E/A) and the interaction distance (C/A). A set of four parametric converger element designs was developed as described in Table 1.

The pre-filmer element is an adaptation of designs commonly used in gas turbines and industrial boilers (5). The liquid fuel is injected tangentially into a recessed groove (Figure 3). The axial dimension of the groove should be large enough to permit the liquid film to homogenize before being exposed to the high-speed gaseous core flow. The film is then circumferentially accelerated as the groove diameter narrows to the main gas port diameter. The characterized dimensions of the pre-filmer are the oxidizer post diameter (A), the diameter (E) and length (F) of the pre-filming groove and the length of the interaction section (C). The diameter (D) and quantity of fuel injection orifices are important, as with the other designs. The key characteristic ratio to be considered is the interaction distance (C/A), although the ratio between the oxidizer post diameter and the dimensions of the pre-filmer groove (E and F) may also be important. Only two parametric pre-filmer element designs were developed as described in Table 1.

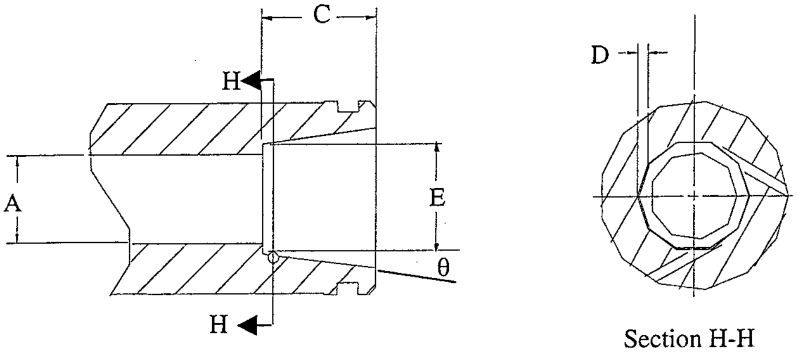

Figure 1: Schematic of Diverger Gas-Centered Swirl Coaxial Injector

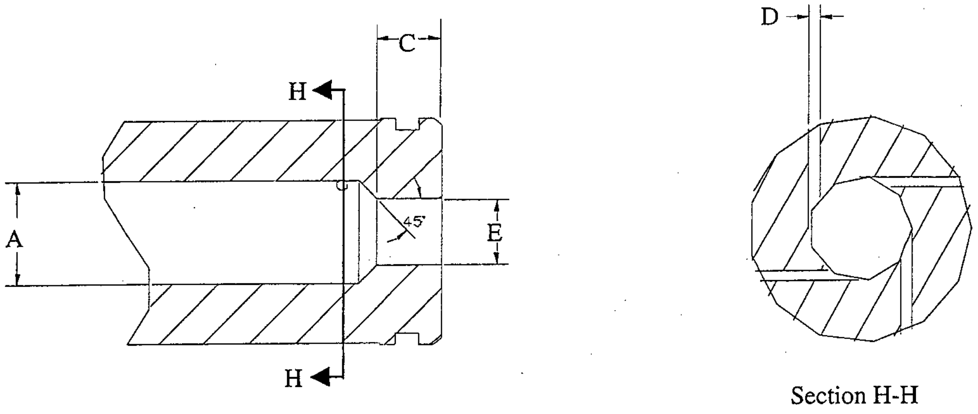

Figure 2: Schematic of Converger Gas-Centered Swirl Coaxial Injector

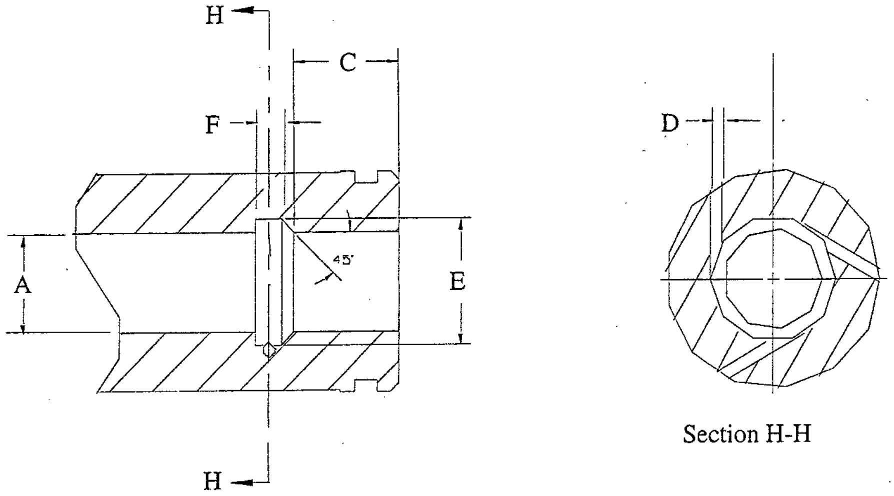

Section H-H

Figure 3: Schematic of Pre-filmer Gas-Centered Swirl Coaxial Injector

Table 1: Characteristic Dimension of Elements (in inches)

DASH #	TYPE	A	C	θ (deg)	D	E	F
1	Diverger	0.400	0.525	0	3 @ 0.047	0.503	-
2	Diverger	0.400	0.525	7	3 @ 0.047	0.503	-
3	Diverger	0.400	0.525	13.65	3 @ 0.047	0.503	-
4	Diverger	0.400	0.325	0	3 @ 0.047	0.503	-
5	Diverger	0.250	0.375	0	3 @ 0.047	0.353	-
6	Pre-filmer	0.400	0.400	-	3 @ 0.047	0.503	0.103
7	Pre-filmer	0.400	0.200	-	3 @ 0.047	0.503	0.103
8	Converger	0.400	0.250	-	3 @ 0.047	0.250	-
9	Converger	0.400	0.250	-	3 @ 0.047	0.125	-
10	Converger	0.400	0.250	-	4 @ 0.041	0.250	-
11	Converger	0.400	0.325	-	3 @ 0.047	0.250	

The parametric element designs were developed using some simple common constraints. The nominal fuel injection pressure drop was set at 20% of the chamber pressure, i.e. 300 psid. This value was chosen to ensure that the fuel injection process was decoupled from the combustion process. In order to keep the nominal fuel injection pressure drop constant, the fuel injection orifice diameter changed as the fuel injection orifice quantity varied. The oxidizer post inlet diameter was selected so the nominal GOX velocity was approximately 200 ft/s. This value was selected to reduce the likelihood of fires initiated by particle-impact in the high pressure GOX system. Subsequent analyses have shown that this value was too low, since it resulted in low injection pressure drops (20-30 psid) in many of the injector designs.

The subject uni-element testing used full-scale AFT element concepts (400 lb_f) integrated into the AFRL uni-element test rig. Cold flow testing was performed in the Area 1-14 High Pressure Cold-Flow Facility while hot fire testing was performed in EC-1 using a workhorse uni-element test rig. This heat-sink design (Figure 4) is based on the Penn State University uni-element diagnostic engine design. The design includes several modular segments held together in a hydraulic ram. The segments include the injector, windowed test segment, barrel extension segment with igniter, two additional barrel segments and the convergent-divergent nozzle segment (from left to right in Figure 4). The windowed section has been replaced with a straight spacer section during these initial characterization experiments. Future experiments are planned using the windowed section to gain access to the interior engine flow characteristics. Ignition is achieved using a hydrogen-oxygen torch that does not run during main-stage engine operation.

A benefit of this engine design is that engine length (L') changes are very straight forward. The majority of testing, including all of the results presented in this paper, have been conducted with L'=8 in.

The interior cross-section of this engine is a 2 inch square. This large chamber facilitates access for optical diagnostic; however, it also result in an extremely large contraction ratio ($A_{chamber}/A_{throat} = 26$).

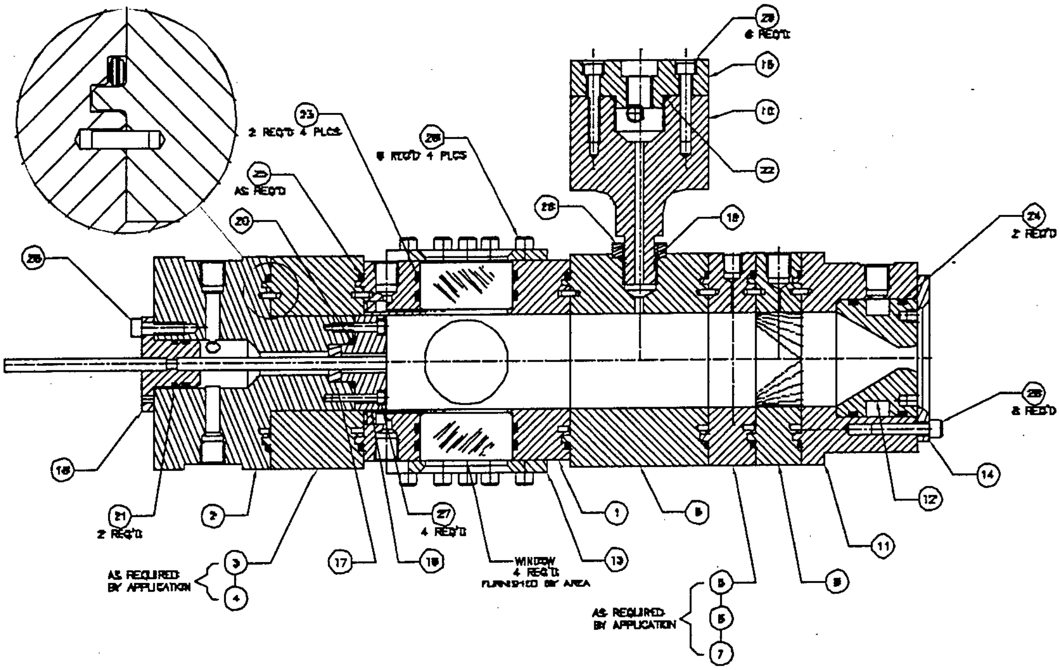

Figure 4: Basic Layout of EC-1 Uni-Element Test Rig

In order to facilitate testing, Sierra Engineering designed an alternative injector segment that could be used in both the EC-1 test rig and the 1-14 High Pressure Cold-Flow facility. The injector assembly includes a copper injector body and oxidizer manifold closeout, a copper test element and a nickel 200 retainer plate. Monel 400 fittings and Viton o-rings were used on the oxidizer system for GOX compatibility. External ports are included to feed the propellants and measure the oxidizer feed pressure.

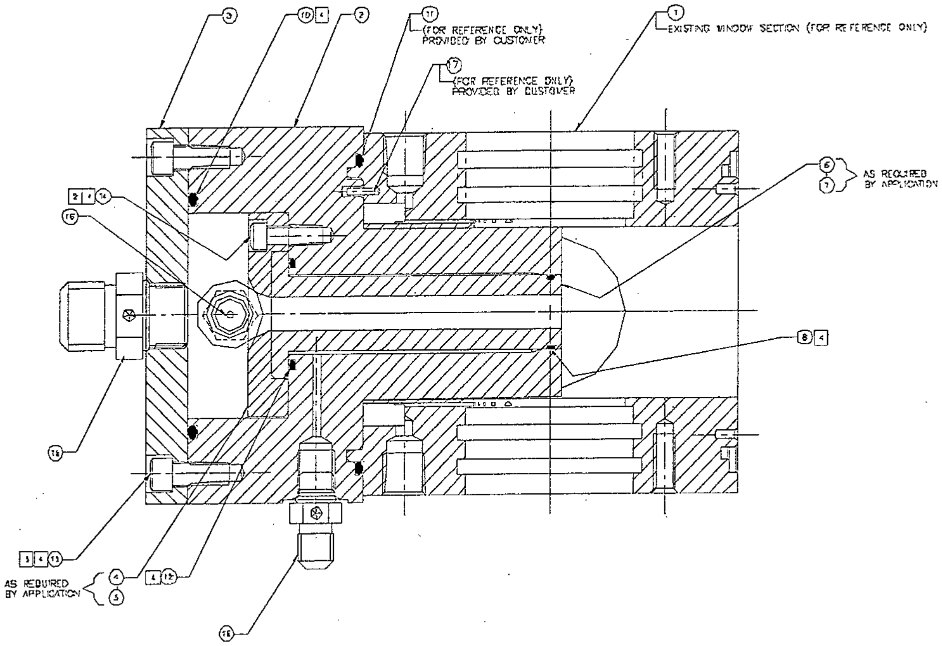

Figure 5: Detail of Sierra Uni-Element Test Injector Assembly

COLD FLOW TEST RESULTS

Cold flow testing was performed at the AFRL High Pressure Cold-Flow Facility located in Area 1-14 at Edwards AFB. The testing used water to simulate the liquid fuel gaseous nitrogen to simulate GOX. The cold flow tests were performed in a vessel pressurized with gaseous nitrogen. The vessel design allows the back-pressure to be adjusted and includes windows for optical access. The diagnostics utilized for this study included back-lit strobe imaging of the spray, mechanical patternation for measurement of liquid flux distribution and phase Doppler interferometry for droplet size and velocity measurement. The mechanical patternator in this system is a linear array, but the injector can be rotated and traversed across the patternator to fully characterize the circumferential spray distribution generated by an injector element. The axial station for all diagnostics can be varied between 1 and 6 inches downstream of the injector exit, although most of the subject test data was collected at 2.0 inches downstream of the injector exit.

The cold flow test conditions were designed to simulate the hot fire operating conditions with respect to the propellant conditions at the point of injection. The cold flow injector operating conditions were designed to match to the hot fire operating condition in the following manner. First, the gas injection velocity was set to the corresponding hot fire operating condition. Second, the injected gas density was matched to the hot fire operating condition based on chamber back-pressure. Since the density of ambient temperature nitrogen and oxygen are very similar, the second condition is achieved with only a slight variation in chamber back-pressure relative to the hot fire chamber pressure. With oxidizer injection velocity and density equivalent to the hot fire case, the final adjustment was to match the hot fire gas-to-liquid momentum ratio by adjusting the mass flow rate of liquid water. Using the above matching conditions, the injectors were tested at chamber pressures ranging from 271 to 1128 psia. These pressures correspond to 250 psia and 1000 psia hot-fire conditions. Selected elements were also tested over a range of injected mixture ratios. The cold flow analog to the 1500 psia hot fire chamber pressure, 1700 psia, was not tested. A comparison of several hot fire operating conditions and the analogous cold flow simulation operating conditions is included as Table 2.

Table 2: Comparison of Element Operating Conditions, Hot Fire to Cold Flow (Hot-Fire MR=2.8)

HOT FIRE (BUTANE/GOX)								***COLD FLOW (H_2O/gN_2)***					
Pc (psia)	Fvac (lbf)	Mdot O (lb/s)	Mdot F (lb/s)	Voj (m/s)	VFj (m/s)	mVo/ mVj	Vo/ Vf	Pc (psig)	Voj (m/s)	mdot N2 (lb/s)	Vf (m/s)	mdot H2O (gpm)	MR
250	333	0.858	0.306	43.0	14.0	8.57	3.6	271	43.0	0.17	10.7	0.582	*2.13*
500	667	1.715	0.613	43.0	28.1	4.28	1.8	557	43.0	0.34	21.4	1.164	*2.13*
750	1000	2.573	0.919	43.0	42.2	2.86	1.2	842	43.0	0.51	32.1	1.746	*2.13*
1000	1333	3.431	1.225	43.0	56.2	2.14	0.9	1128	43.0	0.69	42.8	2.328	*2.13*
1500	*2000*	*5.146*	*1.838*	*43.0*	*84.4*	*1.43*	*0.6*	*1700*	*43.0*	*1.03*	*64.2*	*3.492*	*2.13*

It should be noted that all of the chamber pressures examined in the cold flow testing are subcritical relative to the fuel stimulant (water); however, many of the hot fire operating conditions are supercritical relative to the actual fuels planned for the AFT tests. Because of the difference in the properties of sprays and jets under subcritical and supercritical conditions, one must be careful in the interpretation of these results. Under supercritical conditions, droplets do not exist. However, it is believed that droplet sizes measured under subcritical conditions correspond to the size of structural features found in supercritical conditions. Thus, smaller drop sizes in the subcritical conditions will correspond to smaller structural length scales under supercritical conditions. This will result in an increase in the amount of surface area available for mixing to occur. It is also likely that the mass flux distribution pattern measured in the subcritical, cold flow tests will have a smaller spatial distribution, i.e., there will be less smearing, than would under supercritical conditions. Similar results have been seen in Chehroudi *et al.* (8) where it was found that the spreading rate of a supercritical jet is significantly larger than that for subcritical jets. The increased spreading rate, combined with the lack of a latent heat of vaporization in the supercritical condition will likely yield an increase in mixing over the subcritical case.

Eight of the eleven candidate elements were successfully cold flow tested over a range of operating pressures. The other three elements were not tested because of either element machining problems or diagnostic limitations of the facility.

Several different measurements were made of each element's performance characteristics, some qualitative and others quantitative. Back-lit strobe images were used to qualitatively compare the near-field spray patterns of the different injection elements. Tests were run with only the liquid circuit operating and then with both fluid circuits operating. The "liquid only" tests produced a rapidly expanding liquid cone. The cone typically expanded with half-angles exceeding 75° and often wet the injector face plate. However, when the gas and liquid circuits were run simultaneously, the free liquid film was pulled inwards towards the gas core and rapidly entrained. The images for the 333 lb_f equivalent operating condition are presented in Figure 6. The diverger elements (#1, #3 and #4), appear to have a wider spray pattern with relatively large liquid droplets being thrown toward the periphery of the spray, while the pre-filmer and converger elements produce a narrower spray cone with what appears to be finer droplet sizes.

More quantitative measurements were performed using a combination of mechanical patternation and phase Doppler velocimetry. The patternator was designed to measure the axial component of the liquid flux using a linear array of 27 tubes, each 1/4" square. The liquid (and gas) entering the patternator tubes drain into collection bottles where the liquid level was measured using a capacitance probe accurate to ± 2%. Although the gas vents off to a common manifold that connects back to the chamber, the pressure drop through the patternation system only allows about 25% of the gas to pass through the tubes. This generated a partial stagnation region at the entrance of the patternator tubes and prevented some of the smaller droplets from entering the tubes. The larger droplets have enough momentum to pass through the streamlines and enter the tubes. The collection efficiency of the patternator was defined as the ratio of the integrated liquid mass flux to the injected liquid flow rate. The high gas flow rates and injection velocities generated by these swirl coaxial elements combined with the small droplet sizes resulted in measured collection efficiencies were much less than 100%. The measured collection efficiencies were in the range of 22% - 65%.

Droplet size and velocity were measured using a laser-based phase Doppler interferometer. The instrument simultaneously measures the size and velocity of individual droplets as they pass through a 60 μm by 75 μm probe volume. The optical configuration in this experiment was set to measure droplet sizes ranging from 3.8 μm to 440 μm and velocities ranging from -50 m/s to 250 m/s. The average velocity of droplets less than 20 μm in diameter was taken as a good estimate of the average gas-phase velocity (7). The extreme density of the spray prevented phase Doppler measurements at element flows above equivalent thrusts of 333 lb_f. Even at this flow condition data validation rates for droplet sizing were as low as 15% in the center of the spray, where the liquid mass flux was the highest. In comparison, data validation rates as high as 90% were achieved at the edges of the spray. The validation rates for the velocity measurements were much larger than those for the droplet sizing, typically greater than 97% throughout the spray.

In order to account for the low collection efficiency of the mechanical patternator, the raw liquid mass flux data were scaled according to the measured collection efficiency for each radial profile. For example, if the collection efficiency was 50%, the liquid flux data were multiplied by a factor of 2. Radial profiles of liquid mass flux (measured with the patternator) and axial gas velocity measured at 2.0 inches downstream of the injection point are displayed in Figure 7. The patternator collection efficiency is annotated on each plot. All of the sprays appear to have a solid-cone structure with both the gas and liquid circuits flowing. The diverger elements (#1, #3 and #4) generated a significantly wider spray pattern than the converger elements (#8 and #11). The pre-filmer elements tended to generate a more moderate spray pattern in terms of radial spreading rate. These results are consistent with the imaging experiments discussed earlier (Figure 6).

Most of the mass flux patterns appeared to be well behaved, reaching a maximum value at the centerline and falling off with an approximately Gaussian distribution (Figure 8). One exception was the 15° diverger element (#3) that showed a significant asymmetry in the liquid flux distribution. The extent of the asymmetry in the liquid flux of Element #3 was later documented with a series of patternator tests at different circumferential positions at a back-pressure of 857 psia (Figure 8). The symmetry of the liquid flux distribution for Element #3 improved with increasing back-pressure for all of mixture ratios tested.

The conclusions of the cold flow testing, which guided the selection of elements for the initial hot fire testing, were that the element designs which maintain high relative velocity between the gas and liquid film and allow sufficient residence time for liquid stripping and entrainment should perform the best. All element designs produced sprays that were hollow-cone with only liquid flowing, but became solid-cone sprays with both gas and liquid circuits flowing. Additionally, the atomization characteristics of gas-centered coaxial swirl injectors can produce smaller droplet sizes relative to comparable shear coaxial injectors. Except for #3, the injection element concepts produced sprays with adequate symmetry. The diverger and pre-filmer elements provided greater radial spreading of the liquid spray than the converger elements. It was believed that this characteristic could result in improved inter-element mixing and flame-holding during hot fire tests. The diverger elements also had modest injection pressure drop requirements.

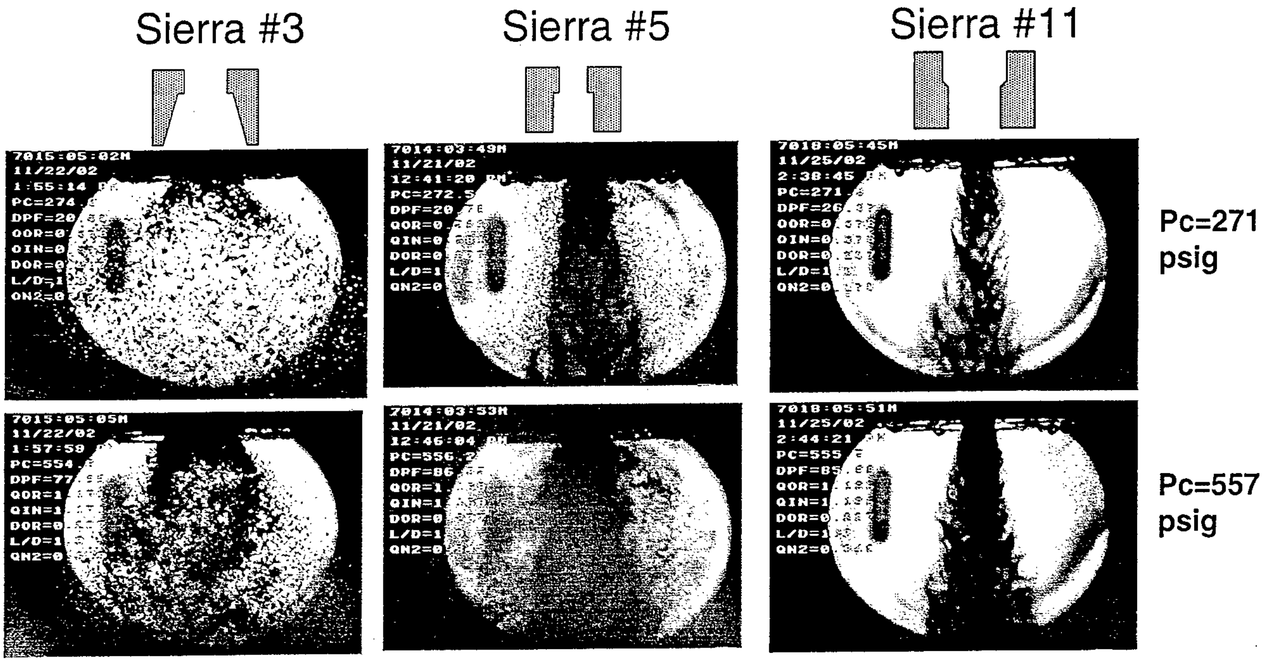

Figure 6: Strobe Back-Lit Images of Three Element Types

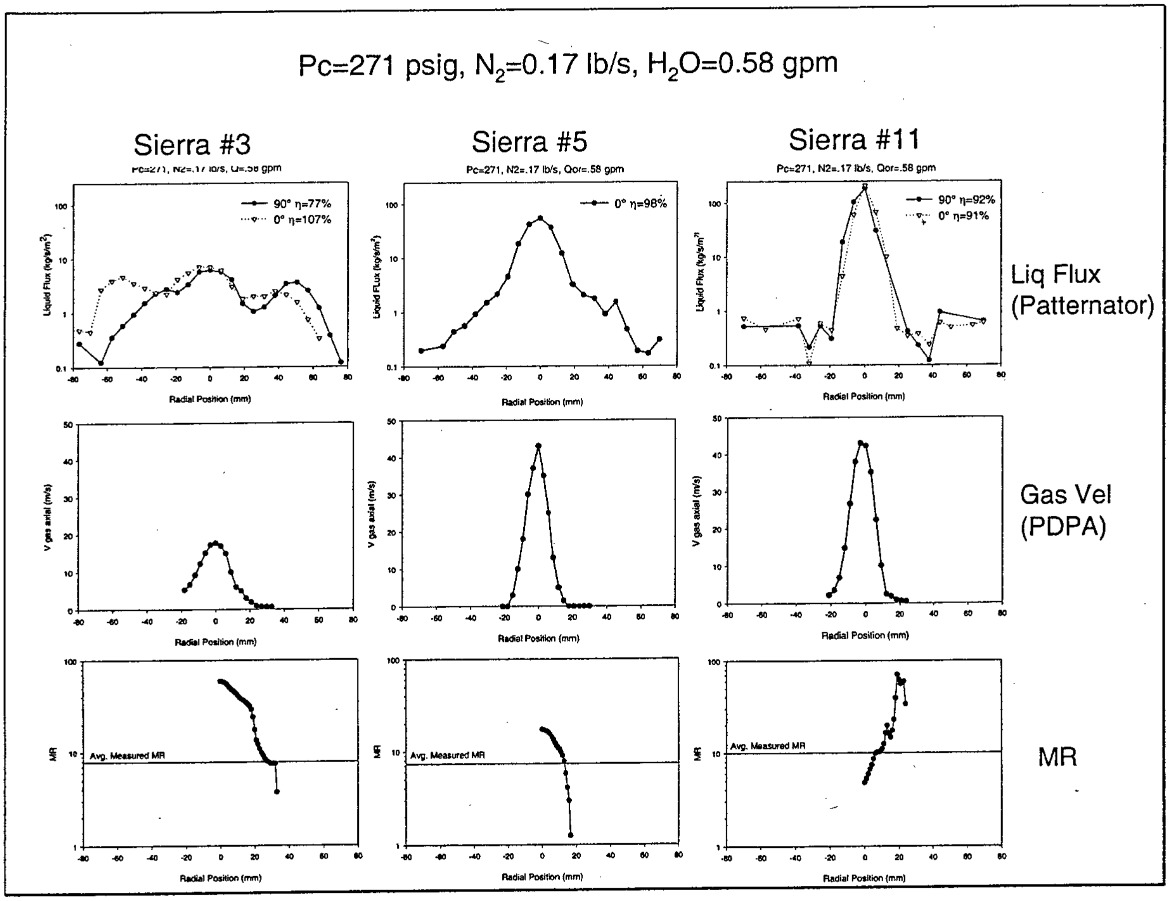

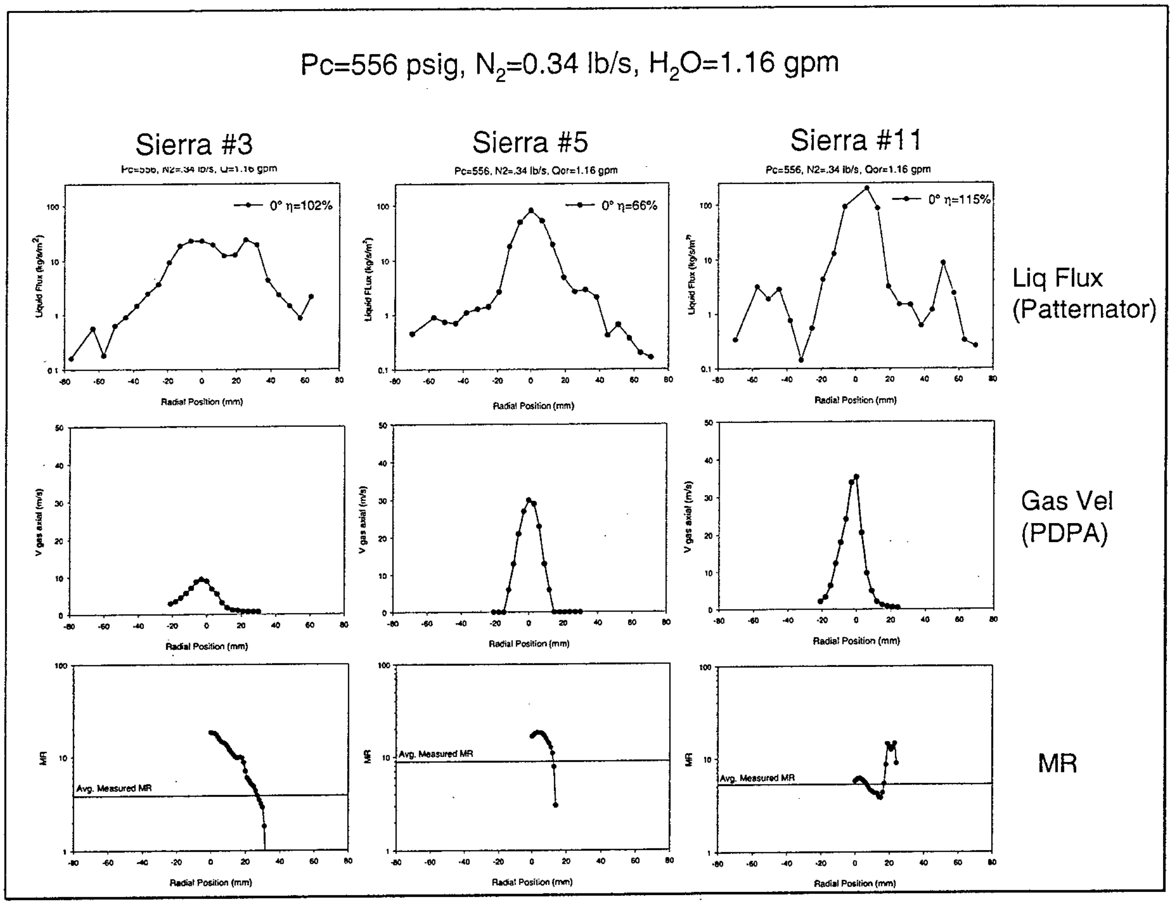

Figure 7: Corrected Liquid Mass Flux, Axial Gas Velocity Profiles and MR

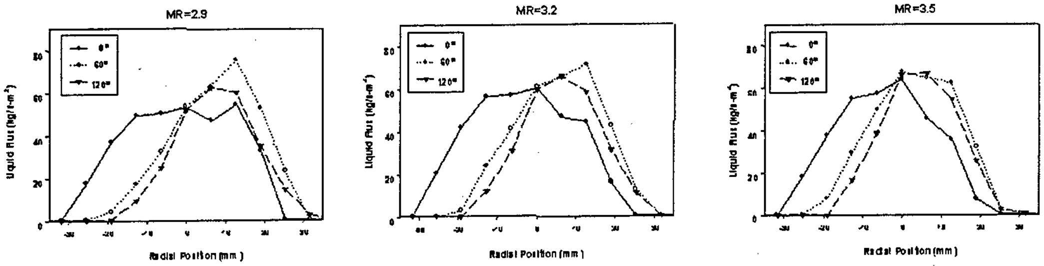

Figure 8: : Influence of Injector Orientation on Measured Gas and Liquid Flux Profiles for Element #3 at Operating MRs of 2.9 (l), 3.2 (c) and 3.5 (r). Operating Chamber Pressure is 857 psi.

HOT FIRE TEST RESULTS

Nearly 400 separate firings were conducted of the various elements. Chamber pressures have ranged from 200 psia to in excess of 1000 psia. All testing described herein has been with Butane as a fuel. Testing is currently underway examining several of these injectors with RP-1 and other hydrocarbon fuels. The elements tested have included several of each of the styles: convergers, divergers, and prefilmers. Figure 9 shows chamber pressures and mixtures ratios evaluated thus far.

The hot fire data used to characterize the elements include characteristic velocity (C*), heat load and chug stability. The C* efficiency measurements presented are the results from a quick-look analysis of the data. Heat loss to the walls and other losses are not taken into account. However, it is reasonable that these losses will be similar between the different injectors and allows for comparison between the elements. An examination of the random measurement errors shows that, although the error bands for the different injectors do have some overlap, the trends related to injector performance can be seen. The random error in the chamber pressure measurement is ±0.1% of the full scale output of the transducer. This nominally corresponds to ±0.7% of the measured pressure. Flowrates are accurate to ±1% of the measured flowrate for the oxidizer and ±0.4% of the measured value for the fuel. The error in the area measurement is less then ±0.5%. This results in an overall uncertainty less then ±1.4%.

Figure 10 shows a comparison of several of the element types at nominal pressure of 500 psi. The converger element resulted in the highest C* efficiency. Qualitatively, one would expect that this element would have a high heat load due to the mixing and burning that likely occurs within the cup. This was borne out in the heat markings seen on the element. However, the heat loads were not high enough to damage the element. The C* efficiency increases with increasing MR, and increased oxidizer injection velocity. This injector has shown no signs of chug instability. The cold flow data shows that this element produces a homogeneous, narrow core, which is consistent with high performance. The high injection pressure drop is consistent with chug stable operation.

The pre-filmer element demonstrated lower performance then the converging design. However, this element showed the most heat marking. In fact, the marking was so severe, testing was not conducted at chamber pressures exceeding 500 psi.

The diverging designs showed the lowest performance. These designs also showed evidence of a chamber oscillation at approximately 200 Hz. Due to the high pressure drop, it is believed that this is not a chug instability. Investigations are underway to find the cause of this oscillation.

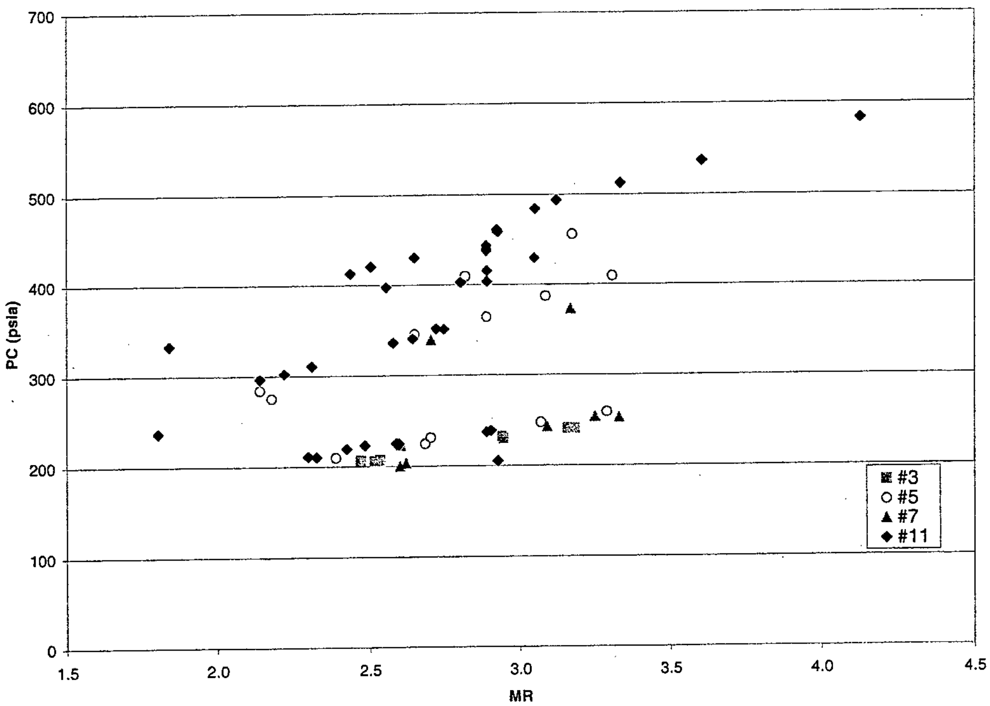

Figure 99: Map of PC-MR Hot Fire Test Conditions

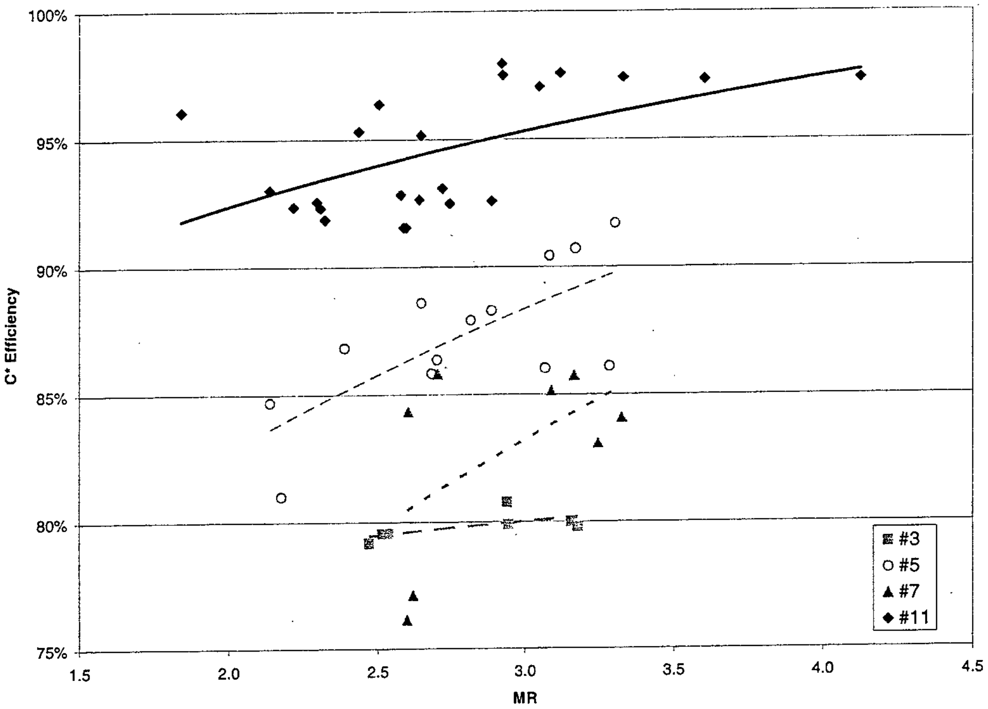

Figure 100: C* Efficiency versus MR for Diverger (#3 and #5), Pre-filmer (#7) and Converger (#11) Elements

SUMMARY

Sierra Engineering and the Air Force Research Laboratory are developing design guidelines for gas-centered swirl coaxial elements. The design methodology is general enough that it can be applied to the development of other novel injector designs. Three basic element concepts have been identified. A set of parametric injection elements has been designed in an effort to identify key design features and acceptable parameter values. Detailed cold flow testing was performed on each of the elements with the hope of identifying remarkable injector characteristics. The cold flow data shows that key design features must be observed for the elements to produce reasonably uniform mass distributions and atomization. The injection pressure drop characteristics are more complex than initially assumed, and the hot fire data indicates that this is an important feature for stable operation. At the pressures tested to date, the element designs appear to have markedly different performance and chug stability characteristics. Ongoing testing will verify these trends, and hopefully identify key design features. As expected in the beginning, the ultimate injection element design will be a compromise of performance, thermal compatibility and combustion stability.

REFERENCES

1. Emission Reduction Through Chemical Kinetic Modeling of Real Engine Effects (REE), Contract F04611-01-C-0010
2. Muss, J.A. and Meagher, G.M.; "Swirl Coaxial Injector Element Characterization for Booster Engines", 1988 Advanced Earth-to-Orbit Propulsion Technology Conference, May, 1988

3. Bailey, T.E, Colbert, J.E. and Mosier, S.A.; FLOX/methane pump-fed engine study, Pratt & Whitney Aircraft, PWA-FR-3040, May, 1969.

4. Oelefein, J.C. and Yang, V.; A Comprehensive Review of Liquid-Propellant Combustion Instabilities in F-1 Engines. Interim Version, Propulsion Engineering Research Center, Penn State University, 23 July 1992.

5. Lefebvre, A.; Atomization and Sprays. Hemisphere Publishing Corp, 1989.

6. Doumas, M. and Laster, R.; "Liquid-Film Properties for Centrifugal Spray Nozzles", *Chemical Engineering Progress*, Vol. 49, No. 10, Oct. 1953.

7. Strakey, P.A., Talley, D.G., Tseng, L.K., and Miner, K.I., "The Effects of LOX Post Biasing on SSME Injector Wall Compatibility," *Journal of Propulsion and Power,* vol 18, no 2, pp 240-246, March-April 2002.

8. Chehroudi, B., Talley, D.G., and Coy, E.; "Visual Characteristics and Initial Growth Rates of Round Cryogenic Jets at Subcritical and Supercritical Pressures," *Physics of Fluids*, Vol. 14, No. 2, 2002.

9. Cheng, G., Johnson, C.W. and Muss, J.A.; "Swirl Coaxial Injector Development Part II - CFD Modeling", 38th JANNAF Combustion Subcommittee Meetings, Destin, FL, 8-12 April, 2002